R&D NOTE

# Improved Recursive Algorithm for Calculation of Probability Density in Breakup Models

**Kiyanoosh Razzaghi and Farhad Shahraki**
Dept. of Chemical Engineering, University of Sistan and Baluchestan, Zahedan 98164-161, Iran

*DOI 10.1002/aic.12393*
*Published online October 19, 2010 in Wiley Online Library (wileyonlinelibrary.com).*

*Keywords: mixing, multi-phase flow, turbulence*

## Introduction

Modeling the breakup of fluid particles in turbulent flows plays a central role in chemical engineering. A very large amount of contributions are proposed to model the breakup mechanism that can mainly be classified as algorithmic models[1–3] and phenomenological models.[4–9] Among these models, phenomenological models have received extensive interest from researchers over the years. However, uncertainties regarding the reliability of such models lead to quite different forms of breakage functions when similar physical arguments are used.[10] The model proposed by Luo and Svendsen[5] was quite different from other models since it needs no adjustable or experimentally-determined parameter. This model was based on the theories of isotropic turbulence and probability, and has been widely used in recent years.[11–14] Based on the same framework, several attempts to improve this model have been appeared in the literature.[7–10,15] Among these works, Kostoglou and Karabelas[10] proposed a unified framework for the derivation of breakage functions based on the statistical description of isotropic turbulence. A literature review on the existing theoretical breakup models can be found in a recent article by Liao and Lucas.[16]

One of the main drawbacks in breakup modeling is the calculation of breakup rate and daughter-size distribution, which are time-consuming because a triple integral is involved in the governing equations, and, therefore, the need for an efficient algorithm to calculate the integrals appeared in the model is essential. This has led to the development of numerical algorithms over the last few years.[17–22] Among these algorithms, the one proposed by Wang and coworkers[21] has received many interest as can be seen in the literature.[10,23–25] The algorithm uses a recursive procedure to calculate the breakup probability density, which reduces the triple integral into a double integral by introducing a cutoff energy as the upper limit of integration. The accuracy of the solution depends severely on the discretization of breakage fraction.

An improved recursive algorithm to calculate the probability density in breakup models is presented. The modified algorithm gives considerably faster solutions than the one proposed by Wang et al.[7] A structured discretization is also used for breakup fraction which significantly improved integration accuracy and computational efficiency.

## Improved Recursive Algorithm

The probability density for a fluid particle with size $d$ breaking with breakup fraction $f_v$, when hit by an eddy of size $\lambda$ can be expressed as

$$P_B(f_v|d,\lambda) = \int_0^\infty P_B(f_v|d,e_\lambda,\lambda)P_e(e_\lambda)\mathrm{d}e_\lambda \tag{1}$$

The upper integration limit can be replaced by a cutoff energy $e_{\lambda,\mathrm{cutoff}}$, which was set to be $10\bar{e}_\lambda$ by Wang et al.[21] and the lower limit of integration should be replaced by the critical eddy energy, which is the minimum eddy energy that can lead to a breakage event,[10] and can be obtained from the solution of equation $f_{v,\min}(e_{\lambda,\mathrm{crit}}) = f_{v,\max}(e_{\lambda,\mathrm{crit}})$. The minimum and maximum breakup fractions can be calculated from capillary pressure constraint and surface energy increase constraint, respectively. The breakup probability distribution according to Wang et al.[7] is written as

$$P_B(f_v|d,e_\lambda,\lambda) = \begin{cases} \frac{1}{f_{v,\max}-f_{v,\min}}, & f_{v,\max}-f_{v,\min} \geq \delta \\ & \text{and } f_{v,\min} < f_v < f_{v,\max} \\ 0, & \text{else} \end{cases} \tag{2}$$

where $\delta$ is a parameter having a small value to avoid singularity. Although the authors assumed that small eddies

Correspondence concerning this article should be addressed to F. Shahraki at fshahraki@eng.usb.ac.ir.

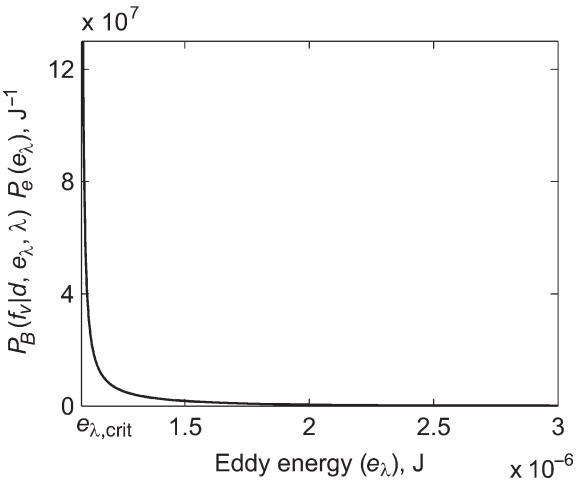


**Figure 1. Variation of the integrand with eddy energy.**

$d = 0.006$ m, $\lambda/d = 0.7$, $\varepsilon = 1$ m$^2$/s$^3$, $\sigma = 0.0725$ N/m and $\delta = 0.001(e_{\lambda,\text{crit}} = 1.0844 \times 10^{-6}$ J).

have almost no effect on breakup, but (as denoted by Kostoglou and Karabelas[10]) it tends to reduce the breakage rate since the lower limit is now obtained from the solution of $f_{v,\max}(e_{\lambda,\text{crit}}) - f_{v,\min}(e_{\lambda,\text{crit}}) = \delta$.

The eddy-energy distribution $P_e(e_\lambda)$ as proposed by Angelidou et al.[26] decreases exponentially with $\lambda$

$$P_e(e_\lambda) = \frac{1}{\bar{e}_\lambda}\exp(-e_\lambda/\bar{e}_\lambda) \tag{3}$$

where $\bar{e}_\lambda = \pi\lambda^3\rho_c\bar{u}_\lambda^2/12$ is the mean kinetic energy of the eddies. Figure 1 shows variation of the integrand $P_B(f_v|d, e_\lambda, \lambda)P_e(e_\lambda)$, with $e_\lambda$ in the range $e_{\lambda,\text{crit}} \le e_\lambda \le e_{\lambda,\text{cutoff}}$. As can be seen, the integrand has a very slow slope in a wide range of eddy energies and grows steeper as $e_\lambda$ approaches $e_{\lambda,\text{crit}}$. The algorithm used by Wang et al.[21] uses rectangular segmentations to calculate $\int_{e_{\lambda,i-1}}^{e_{\lambda,i}} P_B(f_v|d, e_\lambda, \lambda)\ P_e(e_\lambda)\text{d}e_\lambda$ (Figure 2a), while considering the shape of the integrand in the range $e_{\lambda,\text{crit}} \le e_\lambda \le e_{\lambda,\text{cutoff}}$, use of structured trapezoidal segmentations (Figure 2b) can significantly improve integration accuracy and computational efficiency, since in Wang's algorithm, the integrand needs to be calculated at point $i - 1/2$ (surface energy-controlled region), or $i + 1/2$ (capillary pressure-controlled region), which requires iterative procedure. Having chosen discretization points for $f_v$, the modified recursive algorithm of Wang et al.[21] can be treated as follows.

### *Surface energy-controlled region*

In this region, only eddies with kinetic energy larger than $c_f\pi d^2\sigma$ can cause breakup with breakup fraction $f_v$.[21] The probability density is calculated recursively from $f_{v,N} = 0.5$ to $f_{v,c}$ as follows

$$P_B(f_{v,N}|d,\lambda) = \begin{cases} \int_{e_{\lambda,N}}^{e_{\lambda,\text{cutoff}}} P_B(f_v|d,e_\lambda,\lambda)P_e(e_\lambda)\text{d}e_\lambda, & e_{\lambda,N} < e_{\lambda,\text{cutoff}} \\ 0, & e_{\lambda,N} \ge e_{\lambda,\text{cutoff}} \end{cases} \tag{4}$$

and

$$\begin{aligned} P_B(f_{v,i-1}|d,\lambda) &= \int_{e_{\lambda,i-1}}^{e_{\lambda,\text{cutoff}}} P_B(f_v|d,e_\lambda,\lambda)P_e(e_\lambda)\text{d}e_\lambda \\ &= \int_{e_{\lambda,i-1}}^{e_{\lambda,i}} P_B(f_v|d,e_\lambda,\lambda)P_e(e_\lambda)\text{d}e_\lambda \\ &\quad + \int_{e_{\lambda,i}}^{e_{\lambda,\text{cutoff}}} P_B(f_v|d,e_\lambda,\lambda)P_e(e_\lambda)\text{d}e_\lambda \\ &= \tfrac{1}{2}(e_{\lambda,i} - e_{\lambda,i-1})\left\{P_B(f_{v,i-1}|d,e_{\lambda,i-1},\lambda)P_e(e_{\lambda,i-1})\right. \\ &\quad \left. + P_B(f_{v,i}|d,e_{\lambda,i},\lambda)P_e(e_{\lambda,i})\right\} + P_B(f_{v,i}|d,\lambda) \end{aligned} \tag{5}$$

with $i = 2,3,\ldots,N$ and $f_{v,c}$ satisfies the equation $c_{f,c}\sigma\pi d^2 = \sigma\pi\lambda^3/(6df_{v,c}^{1/3})$. The probability distribution function is chosen to be constant in $[f_{v,\min}, f_{v,\max}]$ and

$$P_B(f_{v,i}|d,e_{\lambda,i},\lambda) = \begin{cases} \frac{1}{f_{v,i} - f_{v,i,\min}}, & f_{v,i} - f_{v,i,\min} \ge \delta \\ 0, & f_{v,i} - f_{v,i,\min} < \delta \end{cases} \tag{6}$$

where

$$f_{v,i,\min} = \left(\frac{\pi\lambda^3\sigma}{6e_{\lambda,i}d}\right)^3 \tag{7}$$

and

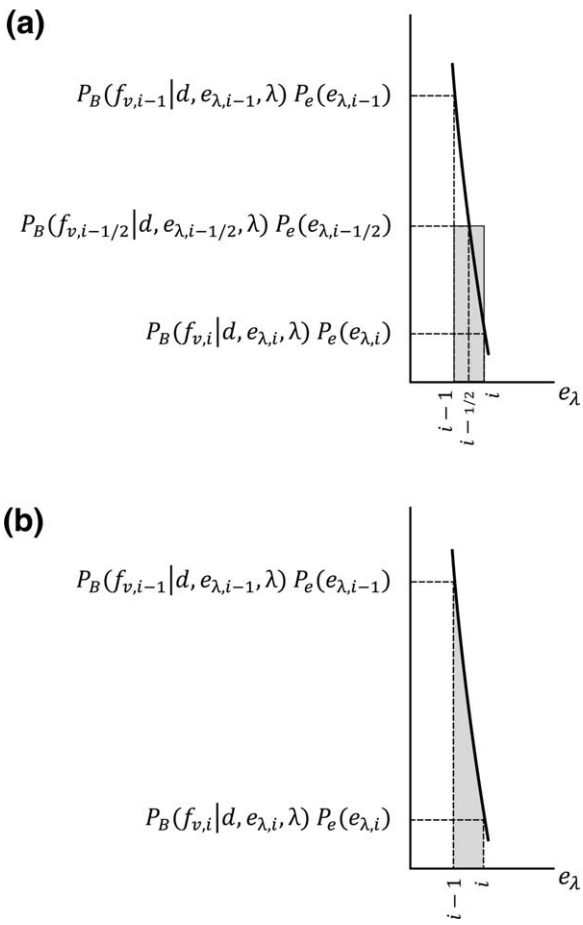


**Figure 2. The methods for the calculation of integral (shaded area).**

(a) Wang et al.[21] and (b) this work.

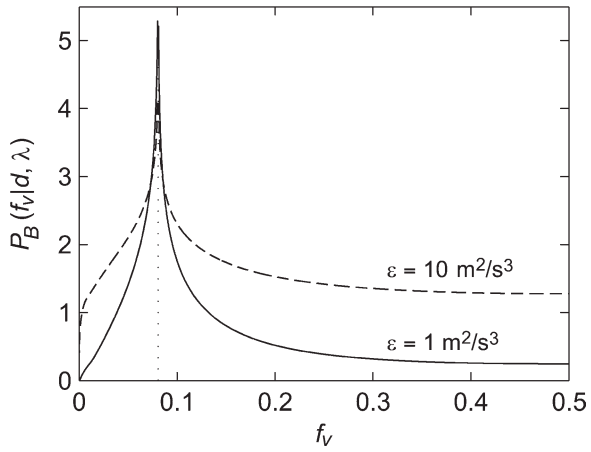


**Figure 3. Effect of energy dissipation rate on the shape of probability density in the vicinity of $f_v = 0$.**

$d = 0.006$ m, $\lambda/d = 0.7$, $\varepsilon = 1$ m$^2$/s$^3$, $\sigma = 0.0725$ N/m and $\delta = 0.001$.

$$e_{\lambda,i} = \left(f_{v,i}^{2/3} + (1 - f_{v,i})^{2/3} - 1\right)\pi d^2\sigma \tag{8}$$

### *Capillary pressure-controlled region*

In this region, only eddies having kinetic energy larger than $\pi\lambda^3\sigma/(6f_v^{1/3}d)$ can cause breakup with breakage fraction $f_v$.[21] The probability density is calculated recursively from $f_{v,0} = 0$ to $f_{v,c}$ as follows

$$P_B(f_{v,0}|d,\lambda) = 0 \tag{9}$$

$$P_B(f_{v,1}|d,\lambda) = \begin{cases} \int_{e_{\lambda,1}}^{e_{\lambda,\text{cutoff}}} P_B(f_v|d,e_\lambda,\lambda)P_e(e_\lambda)\mathrm{d}e_\lambda, & e_{\lambda,1} < e_{\lambda,\text{cutoff}} \\ 0, & e_{\lambda,1} \geq e_{\lambda,\text{cutoff}} \end{cases} \tag{10}$$

and

$$\begin{aligned} P_B(f_{v,i+1}|d,\lambda) &= \int_{e_{\lambda,i+1}}^{e_{\lambda,\text{cutoff}}} P_B(f_v|d,e_\lambda,\lambda)P_e(e_\lambda)\mathrm{d}e_\lambda \\ &= \int_{e_{\lambda,i+1}}^{e_{\lambda,i}} P_B(f_v|d,e_\lambda,\lambda)P_e(e_\lambda)\mathrm{d}e_\lambda \\ &\quad + \int_{e_{\lambda,i}}^{e_{\lambda,\text{cutoff}}} P_B(f_v|d,e_\lambda,\lambda)P_e(e_\lambda)\mathrm{d}e_\lambda \\ &= \tfrac{1}{2}(e_{\lambda,i} - e_{\lambda,i+1})\left\{P_B(f_{v,i}|d,e_{\lambda,i},\lambda)P_e(e_{\lambda,i})\right. \\ &\quad \left. + P_B(f_{v,i+1}|d,e_{\lambda,i+1},\lambda)P_e(e_{\lambda,i+1})\right\} + P_B(f_{v,i}|d,\lambda) \end{aligned} \tag{11}$$

with $i = 1,2, \ldots, N-1$, and the probability distribution function is

$$P_B(f_{v,i}|d,e_{\lambda,i},\lambda) = \begin{cases} \frac{1}{f_{v,i,\max} - f_{v,i}}, & f_{v,i,\max} - f_{v,i} \geq \delta \\ 0, & f_{v,i,\max} - f_{v,i} < \delta \end{cases} \tag{12}$$

where $f_{v,i,\max}$ is found from

$$f_{v,i,\max}^{2/3} + (1 - f_{v,i,\max})^{2/3} - 1 = e_{\lambda,i}/(\pi d^2\sigma) \tag{13}$$

and

$$e_{\lambda,i} = \frac{\pi\lambda^3\sigma}{6f_{v,i}^{1/3}d} \tag{14}$$

Since the modified algorithm have only one iteratively found parameter, i.e. $f_{v,i,\max}$, then it clearly has a computational time less than the one proposed by Wang et al.[21]

## Discretization of $f_v$

Figure 3 shows the effect of energy dissipation rate $\varepsilon$ on $P_B(f_v|d,\lambda)$. The variation of the daughter bubble/droplet size distribution is sharper in small $f_v$ range, especially when the bubble and/or the energy dissipation rate are large. To get a higher accuracy for a given number of $f_v$ divisions, a fine division of $f_v$ is recommended when $f_v$ is small. Since the function $P_B(f_v|d,\lambda)$ is singular around $f_v = f_{v,c}$, thus, the use of a very fine grid for $f_v$ in the vicinity of $f_{v,c}$ can significantly capture the shape of $P_B(f_v|d,\lambda)$ in the region of singularity.[10] Based on these arguments, a structured discretization is used to increase the integration accuracy and saving in computational time. This structure condenses discretization points $f_v$ as it approaches zero and $f_{v,c}$. For three successive points $i-1$, $i$ and $i+1$, the discretization points are obtained as

$$(f_{v,i+1} - f_{v,i})/(f_{v,i} - f_{v,i-1}) = k \tag{15}$$

or

$$f_{v,i+1} - (k+1)f_{v,i} + kf_{v,i-1} = 0 \tag{16}$$

with $i = 1,2, \ldots, M-1$. For the capillary pressure-controlled region $f_{v,0} = 0$ and $f_{v,M} = f_{v,c}$, and for the surface energy-controlled region $f_{v,0} = f_{v,c}$ and $f_{v,M} = 0.5$. The parameter $k$ is defined as

$$k = 1 + p$$

in the surface energy controlled region, and

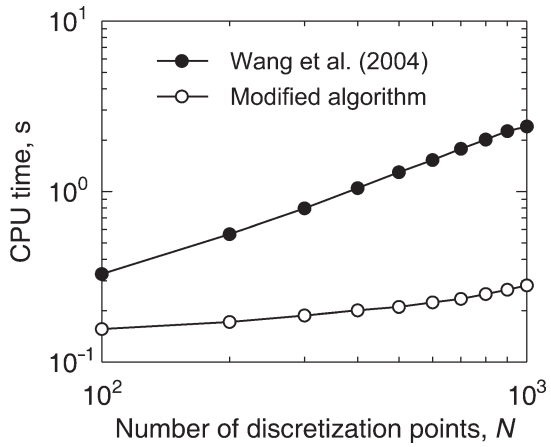


**Figure 4. Comparison of CPU time between Wang's algorithm and modified algorithm as number of discretization points increases.**

Table 1. Values of $P_B(f_v|d, \lambda)$ Near the Singularity Point ($f_{v,c} = 0.0808$)[†]

| | Number of discretization points ($N$) | | | | |
|---|---|---|---|---|---|
| $d = 0.006$ m | 200 | 400 | 600 | 800 | 1000 |
| Wang's algorithm | 5.0061 | 5.1876 | 5.2272 | 5.2788 | 5.2811 |
| | (0.7344)[‡] | (1.3125) | (1.9063) | (2.5156) | (3.0469) |
| Improved algorithm | 5.2915 | 5.2861 | 5.2829 | **5.2811** | **5.2811** |
| | (0.0313) | (0.0469) | (0.0781) | (0.1094) | (0.1406) |
| $d = 0.002$ m | | | | | |
| Wang's algorithm | 0.0694 | 0.0723 | 0.0737 | 0.0742 | 0.0750 |
| Improved algorithm | 0.0758 | 0.0752 | 0.0752 | **0.0751** | **0.0751** |

[†]$\sigma = 0.0725$ N/m, $\lambda = 0.7d$ and $\varepsilon = 1$ m$^2$/s$^3$ ($\delta = 0.001$).
[‡]CPU time in seconds.

$$k = \begin{cases} 1 + \eta p, & 0 \le f_v \le f_{v,c}/2 \\ 1 - p, & f_{v,c}/2 < f_v \le f_{v,c} \end{cases}$$

in the capillary pressure controlled region, where $0 \le p < 1$ and $\eta \ge 0$ are grid controlling parameters. $\eta$ depends on the shape of $P_B(f_v|d, \lambda)$, and, therefore, on the energy dissipation rate. As the energy dissipation rate increases, discretization points need to become more dense in the vicinity of $f_v = 0$ (Figure 3). Values of $\eta$ greater than unity condense discretization points more rapidly as $f_v$ approaches zero. Large values of $\eta$ result in sharp condensing of discretization points toward zero, while very small values of $\eta$ result in sharp condensing toward $f_{v,c}$. When $p = 0$, equal-size discretization points are achieved.

## Algorithm Efficiency

To evaluate the efficiency and strength of the presented algorithm, the integral of Eq. 1 is evaluated by the improved algorithm with different values of $N$. The integral is calculated on a Pentium® 4, CPU 3 GHz and 512 MB of RAM. Figure 4 shows CPU time needed to calculate the integral. The modified algorithm uses structured discretization while Wang's algorithm uses equal-size discretization. Evidently, by increasing the number of subregions, the difference in computational time for the two algorithms increases. However, as the figure shows, the modified algorithm is considerably faster than the one proposed by Wang et al.[21] approximately in the order of $10^{-1}$ s.

Considering the segmentation schemes, both methods have a global truncation error of order $h^2$.[27,28] Having chosen small values of $h$, both methods will have the same required accuracy (often 3–4 significant digits), although the maximum global error associated with trapezoidal segmentation is twice the rectangular segmentation (see the Appendix). It is obvious that both methods will give the same result, except at the points close to the singularity. As the grid becomes denser, on the one hand the correct shape of $P_B(f_v|d, \lambda)$ is followed closer, and on the other any discrepancy is restricted to a smaller domain, leading to a smaller overall error.[10] Table 1 provides values of $P_B(f_v|d, \lambda)$ near the singularity point for the two methods. Since the trapezoidal segmentation overestimates the sections area, increasing the discretization points helps the overestimation to be compensated, but the rectangular segmentation, on the other hand, underestimates and the area increases by increasing $N$. For $d = 0.006$ m, the improved algorithm reaches the required precision by 600 points; however, this can be reached by a 1,000 points by the Wang's algorithm. This can also be seen for $d = 0.002$ m where in this case the Wang's algorithm needs 1,000 points to reach the value of 0.0751.

## Notation

$c_f$ = parameter of surface energy increase, $f_v^{2/3} + (1 - f_v)^{2/3} - 1$
$d$ = diameter of mother bubble/drop, m
$e_\lambda$ = kinetic energy of an eddy with size $\lambda$, J
$\overline{e}_\lambda$ = mean kinetic energy of an eddy with size $\lambda$, J
$f_v$ = breakup fraction
$h$ = step size
$k$ = discretization parameter
$N$ = number of discretization points
$p$ = discretization parameter
$P_B(f_v|d, \lambda)$ = probability density function
$P_B(f_v|d, e_\lambda, \lambda)$ = bubble/drop probability distribution function
$P_e(e_\lambda)$ = energy distribution function of an eddy with size, J$^{-1}$
$\overline{u}_\lambda$ = mean velocity of an eddy with size, m s$^{-1}$

### *Greek letters*

$\delta$ = parameter of the Wang's model
$\varepsilon$ = energy dissipation rate, m$^2$ s$^{-3}$
$\eta$ = discretization parameter
$\lambda$ = eddy size, m
$\rho_c$ = density of continuous phase, kg m$^{-3}$
$\sigma$ = surface tension, N m$^{-1}$

## Literature Cited


1. Valentas KJ, Bilous O, Amundson NR. Analysis of breakage in dispersed phase systems. *Ind Eng Chem Fundam.* 1966;5:271–279.
2. Kostoglou M, Karabelas AJ. On the steady state size distribution of dispersions in breakage processes. *Chem Eng Sci*. 1997;52:1285–1299.
3. Diemer RB, Olson JH. A moment methodology for coagulation and breakage problems: Part 3-generalized daughter distribution functions. *Chem Eng Sci*. 2002;57:4187–4198.
4. Tsouris C, Tavlarides LL. Breakage and coalescence models for drops in turbulent dispersions. *AIChE J*. 1994;40:395–406.
5. Luo H, Svendsen HF. Theoretical model for drop and bubble breakup in turbulent dispersions. *AIChE J*. 1996;42:1225–1233.
6. Martínez-Bazán C, Montanes JL, Lasheras JC. On the breakup of an air bubble injected into fully developed turbulent flow. Part 1. Breakup frequency. *J Fluid Mech*. 1999;401:157–182.
7. Wang T, Wang J, Jin Y. A novel theoretical breakup kernel function for bubbles/droplets in a turbulent flow. *Chem Eng Sci*. 2003;58:4629–4637.
8. Andersson R, Andersson B. Modeling the breakup of fluid particles in turbulent flows. *AIChE J*. 2006;52:2031–2038.
9. Zhao H, Ge W. A theoretical bubble breakup model for slurry beds or three-phase fluidized beds under high pressure. *Chem Eng Sci*. 2007;62:109–115.

10. Kostoglou M, Karabelas AJ. Toward a unified framework for the derivation of breakage functions based on the statistical theory of turbulence. *Chem Eng Sci*. 2005;60:6584–6595.
11. Andersson R, Andersson B, Chopard F, Noren T. Development of a multi-scale simulation method for design of novel multiphase reactors. *Chem Eng Sci*. 2004;59:4911–4917.
12. Chen P, Sanyal J, Duduković MP. Numerical simulation of bubble columns flows: effect of different breakup and coalescence closures. *Chem Eng Sci*. 2005;60:1085–1101.
13. Alopaeus V, Laakkonen M, Aittamaa J. Numerical solution of moment-transformed population balance equation with fixed quadrature points. *Chem Eng Sci*. 2006;61:4919–4929.
14. Li G, Yang X, Dai G. CFD simulation of effects of the configuration of gas distributors on gas-liquid flow and mixing in a bubble column. *Chem Eng Sci*. 2009;64:5104–5116.
15. Hagesaether L, Jakobsen HA, Svendsen HF. A model for turbulent binary breakup of dispersed fluid particles. *Chem Eng Sci*. 2002;57:3251–3267.
16. Liao Y, Lucas D. A literature review of theoretical models for drop and bubble breakup in turbulent dispersions. *Chem Eng Sci*. 2009;64:3389–3406.
17. Kostoglou M, Karabelas AJ. An assessment of low-order methods for solving the breakage equation. *Powder Technol*. 2002;127:116–127.
18. Kostoglou M, Karabelas AJ. Optimal low order methods of moments for solving the fragmentation equation. *Powder Technol*. 2004;143–144:280–290.
19. Attarakih MM, Bart H-J, Faqir NM. Numerical solution of the spatially distributed population balance equation describing the hydrodynamics of interacting liquid-liquid dispersions, *Chem Eng Sci*. 2004;59:2567–2592.
20. Liu Y, Tadé MO. New wavelet-based adaptive method for the breakage equation. *Powder Technol*. 2004;139:61–68.
21. Wang T, Wang J, Jin Y. An efficient numerical algorithm for "A novel theoretical breakup kernel function of bubble/droplet in a turbulent flow". *Chem Eng Sci*. 2004;59:2593–2595.
22. Sommer M, Stenger F, Peukert W, Wagner NJ. Agglomeration and breakage of nanoparticles in stirred media mills-a comparison of different methods and models. *Chem Eng Sci*. 2006;61:135–148.
23. Wang T, Wang J, Jin Y. Theoretical prediction of flow regime transition in bubble columns by the population balance model. *Chem Eng Sci*. 2005;60:6199–6209.
24. Wang T, Wang J, Jin Y. A CFD-PBM coupled model for gas-liquid flows. *AIChE J*. 2006;52:125–140.
25. Coutelieris FA. On the prediction of an average droplet size evolution during transport in homogeneous porous media under laminar flow conditions. *J Porous Media*. 2010;13:195–207.
26. Angelidou C, Psimopoulos M, Jameson GJ. Size distribution functions of dispersions. *Chem Eng Sci*. 1979;34:671–676.
27. Stewart J. *Calculus: Early Transcendentals*. 6th ed. Belmont, CA: Thomson Brooks/Cole; 2007.
28. Murphy J, Ridout D, McShane B. *Numerical Analysis, Algorithms and Computation*. Chichester: Ellis Horwood; 1988.

## Appendix

Choosing $h = (b - a)$ in the integration interval $[a,b]$, the upper bound of the global truncation error $|\varepsilon_G|$ for the two segmentation methods to calculate $\int_a^b f(x)\mathrm{d}x$ becomes[27,28]

$$|\varepsilon_G|_{\text{trapezoidal}} \leq (b-a)\frac{h^2}{12}\max_{a\leq x\leq b}\{|f''(x)|\} \tag{A1}$$

$$|\varepsilon_G|_{\text{rectangular}} \leq (b-a)\frac{h^2}{24}\max_{a\leq x\leq b}\{|f''(x)|\} \tag{A2}$$

Evidently, the global error associated with trapezoidal segmentation is twice the global error associated with rectangular segmentation, but both global errors have order $h^2$. Furthermore, the estimates depend on the size of the second derivative, because $f''(x)$ measures how much the graph is curved (in fact $f''(x)$ measures how fast the slope of $f(x)$ changes). Hence, very large and very small values of $|f''(x)|$ give approximately the same truncation error. Furthermore, the actual error is substantially less than the upper bound of error.

As can be seen in Figure 1, the integrand asymptotically approaches zero (as $e_\lambda \to \infty$), and infinity (as $e_\lambda \to e_{\lambda,\text{crit}}$). The integrand can be approximated as a straight line for $e_\lambda > 1.35 \times 10^{-6}$ J, and in the region near $e_{\lambda,\text{crit}}$. Hence, in these regions both segmentations give negligible truncation error ($f''(x)$ is nearly zero). Therefore, the difference is restricted to a small region in $1.1 \times 10^{-6}$ J $< e_\lambda < 1.35 \times 10^{-6}$ J. Making order-of-magnitude analysis to determine the maximum truncation error in this region, we obtain $(b - a) \sim 10^{-7}$, $h \sim 10^{-9}$ (for 100 discretization points), and $\max_{a\leq x\leq b}\{|f''(x)|\} \sim 10^{20}$. Hence, $|\varepsilon_G|_{\text{trapezoidal}}$ and $|\varepsilon_G|_{\text{rectangular}}$ have order $10^{-5}$. Clearly, the maximum error associated with each method is very small compared with required computational precision (often 3–4 significant digits).

*Manuscript received May 27, 2010, and revision received July 29, 2010.*